Int J Thermophys (2008) 29:505–533
DOI 10.1007/s10765-008-0410-4

Densities and Excess, Apparent, and Partial Molar Volumes of Binary Mixtures of $BMIMBF_4$ + Ethanol as a Function of Temperature, Pressure, and Concentration

I. M. Abdulagatov · A. Tekin · J. Safarov · A. Shahverdiyev · E. Hassel

Received: 27 July 2007 / Accepted: 27 February 2008 / Published online: 18 April 2008

Abstract The densities of five $BMIMBF_4$ (1-butyl-3-methylimidazolium tetrafluoroborate) + ethanol binary mixtures with compositions of (0.0701, 0.3147, 0.5384, 0.7452, and 0.9152) mole fraction $BMIMBF_4$ and of pure $BMIMBF_4$ have been measured with a vibrating-tube densimeter. Measurements were performed at temperatures from 298 K to 398 K and at pressures up to 40 MPa. The total uncertainty of density, temperature, pressure, and concentration measurements were estimated to be less than $0.1\,\mathrm{kg\cdot m^{-3}}$, 15 mK, 5 kPa, and 10^{-4}, respectively. The uncertainties reported in this article are expanded uncertainties at the 95% confidence level with a coverage factor of $k = 2$. The measured densities were used to study derived volumetric properties such as excess, apparent, and partial molar volumes. It is shown that the values of excess molar volume for $BMIMBF_4$ + ethanol mixtures are negative at all measured temperatures and pressures over the whole concentration range. The effect of water content on the measured values of density is discussed. The volumetric (excess, apparent, and partial molar volumes) and structural (direct and total correlation integrals, cluster size) properties of dilute $BMIMBF_4$ + ethanol mixtures were studied in terms of the Krichevskii parameter. The measured densities were used to develop a Tait-type equation of state.

Present Address:
I. M. Abdulagatov (✉)
Physical and Chemical Properties Division, National Institute of Standards and Technology, 325 Broadway, Boulder, Colorado 80305, USA
e-mail: ilmutdin@boulder.nist.gov

A. Tekin
Erciyes University, 38039 Kayseri, Turkey

J. Safarov · A. Shahverdiyev
Azerbaijan Technical University, H. Javid Avenue 25, AZ1073 Baku, Azerbaijan

J. Safarov · E. Hassel
Lehrstuhl für Technische Thermodynamik, Universität Rostock, 18059 Rostock, Germany

Keywords Apparent molar volume · Binary mixture · $BMIMBF_4$ · Density · Direct and total correlation integrals · Ethanol · Excess molar volume · Ionic liquid · Krichevskii function · Partial molar volume

1 Introduction

Thermodynamic properties of mixtures containing ionic liquids (ILs) and alcohols are of technological and theoretical interest. Volumetric properties (density and excess, apparent, and partial molar volumes) of IL-containing mixtures (ILs + organic substances and water) are some of the most important thermodynamic properties. They provide very useful information on the structural and intermolecular interactions between the solvent and solute molecules (or ions) with different sizes, shapes, and chemical nature. Previous studies [1–3] have shown the addition of alcohols into ILs play a dramatic role in their phase behavior. As is well known (see, for example, [4,5]), even small additions of a low molar mass solvent can dramatically increase or decrease the thermodynamic and transport properties relative to the properties of the pure ILs. Although ILs have been widely studied in the literature, information on the thermodynamic properties of pure ILs and their mixtures with organic solvents is very scarce. Moreover, large inconsistencies among the available reported data of pure $BMIMBF_4$ are found in the literature. An analysis of the reported values of the density for pure $BMIMBF_4$ reveals that all the available density data at atmospheric pressure and at temperatures from 298 K to 398 K show a scatter of $\pm 1.1\%$.

Previously the pure-component ($BMIMBF_4$) densities were studied by many authors [6–27]. A majority of the reported density data for $BMIMBF_4$ were measured at atmospheric pressure and at temperatures up to 392 K. Only a few density data sets reported by [6,9,14,16,22] were found in the literature at high pressures (up to 60 MPa) and at temperatures up to 393 K. Various techniques (vibrating-tube densimeter, pycnometer, piezometers, gravimetric analysis) were employed to measure the density of pure $BMIMBF_4$. The uncertainties of the reported data at atmospheric pressure are within 0.1–0.3 $\mathrm{kg \cdot m^{-3}}$ (or 0.011–0.034%). A literature survey revealed that there are no density data for $BMIMBF_4$ + ethanol mixtures. The densities for other binary IL ($BMIMBF_4$)-containing mixtures (water + $BMIMBF_4$ and organic solvent + $BMIMBF_4$, ILs + $BMIMBF_4$, and methanol + $BMIMBF_4$) have been reported by several authors [11,15,22,23,27].

The main objective of this work is to provide new accurate experimental density data for binary $BMIMBF_4$ + ethanol mixtures at temperatures from 298 K to 398 K and at pressures up to 40 MPa over the whole composition range using a vibrating-tube technique. The present results considerably expand the available thermodynamic database for $BMIMBF_4$ + ethanol mixtures and pure $BMIMBF_4$.

2 Experimental

The (P, ρ, T, x) properties of $BMIMBF_4$ + ethanol mixtures were studied using a modified high-pressure, high-temperature Anton-Paar vibrating-tube densimeter

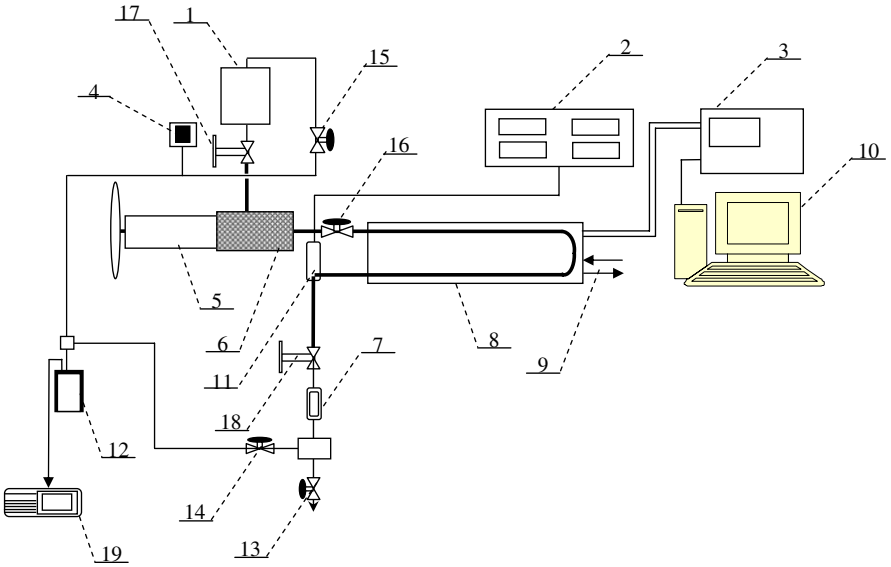

Fig. 1 Vibration-tube densimeter. 1: vessel for the sample; 2; pressure indicator; 3: temperature and frequency control system; 4: vacuum indicator; 5: hand pump; 6: heater; 7: visual window; 8: vibration-tube; 9: water cooling; 10: computer; 11: pressure sensor; 12: thermos for cooling; 13–16: valves; 17, 18: high pressure valves; 19: vacuum pump

(VTD, Model DMA HTP). A schematic diagram of the experimental VTD apparatus is shown in Fig. 1. The core of the apparatus is the VTD. The length of the tube is about 15 cm, the U radius is about 1 cm, the outer diameter is about 6 mm, and the inner diameter is about 2 mm. The volume of the liquid in the tube was 2 cm^3. The tube was made from Hastelloy C-276. The vibrating tube is fixed to the thermostated block of the cell located inside two thermostated jackets. The temperature was maintained constant to 10 mK. The period of oscillation measurement and the temperature control is implemented within the DMA-HDT control system (3), which consists of the measurement cell and a modified DMA 5000 control unit, connected to PC. For the present VTD, the period of vibration is within 2550 µs to 2670 µs. The period of oscillation is measured with an uncertainty of 1 ns. Pressure was created by a hand pump (5) (759.1100-HMEL, SITEC) and measured by a pressure sensor (2) from WIKA Manometer AG, Switzerland. The temperature was measured using the (ITS-90) Pt100 thermometer with an uncertainty of 15 mK. For evacuating the whole apparatus, a vacuum pump (19) (Model ILMVAC GmbH, Germany) is employed.

For this method the density can be written explicitly as

$$\rho = A - B\tau^2, \tag{1}$$

where parameters A and B are both functions of temperature and pressure. The accuracy of the method is limited by the calibration procedure. Usually the temperature and pressure dependences of A and B are determined using the calibration procedures with a minimum of two reference fluids such as water, methanol, benzene, nitrogen,

and toluene whose *PVT* properties are well known and should be performed very carefully. In this work internationally accepted (IAPWS standards) reference density data for water [28] and IUPAC reference data for methanol [29] were used for calculation of the calibration constants A and B as a function of T and P. The parameter B is approximately a linear function of temperature (slope, $(dlnB/dT)$ is about 10^{-4} to $10^{-3}\,\mathrm{K}^{-1}$).

The uncertainty in the pressure measurements is 5 kPa. The uncertainty in the determination of the calibration constant B is within 0.05 and 0.5% depending on the temperature and pressure. The uncertainty in the concentration of the mole fraction was less than 10^{-4}. A detailed uncertainty analysis of the method (all the measured quantities, corrections, and error propagation) showed (see also Abdulagatov et al. [30]) that the uncertainty in density measurements is $0.05\,\mathrm{kg}\cdot\mathrm{m}^{-3}$ at low pressures (near atmospheric pressure) and $0.15\,\mathrm{kg}\cdot\mathrm{m}^{-3}$ at high pressures (the combined expanded uncertainty, coverage factor is $k = 2$). This leads to maximum relative uncertainties of 0.02% for the performed measurements at high temperatures and high pressures and 0.01% at low temperatures and low pressures. The reproducibility of the density measurements is within $\pm 0.01\,\mathrm{kg}\cdot\mathrm{m}^{-3}$ at low pressures and $\pm 0.05\,\mathrm{kg}\cdot\mathrm{m}^{-3}$ at high pressures. The uncertainty in the density of the calibration fluids is 0.001%. To verify the experimental apparatus and calibration procedure, the densities of pure ethanol, benzene, and toluene were measured over the same experimental range for the selected T and P and compared in detail with reported data. We reproduced reference data for ethanol, benzene, and ethanol within an uncertainty of about 0.005–0.015%.

Ionic liquids (stated purity > 98 mass%) were supplied from Solvent Innovation, Germany. Ethanol was supplied from Merck (Germany) with a purity of 99.99 mass% and used without further purification. Twice-distilled water and pure methanol (>99.9 mass%) from Merck, Germany, were used for the calibration of the period of oscillation. The water content in the IL ($BMIMBF_4$) before dehydration was 621 ppm. To reduce the water content and volatile compounds to negligible values, the sample was thoroughly dried before use under a reduced pressure of about 0.05 Pa with heating at $T = 373.15\,\mathrm{K}$ for 48 h. We kept the sample as dry as possible (no contact with air). After this procedure, the water content in the $BMIMBF_4$ was determined with a coulometric "Aquapal" Karl Fischer. The final water content in our ILs sample was quite low (62 ± 10 ppm).

3 Results and Discussion

Measurements of the density of $BMIMBF_4$ + ethanol as a function of temperature, pressure, and concentration were performed at five concentrations of (0.07014, 0.31466, 0.53840, 0.74519, 0.91517) mole fraction of $BMIMBF_4$, along with measurements on pure $BMIMBF_4$, for temperatures between 298.15 K and 398.15 K. The pressure ranged from 0.1 MPa to 40 MPa. The experimental results are presented in Table 1. This table also includes apparent molar volumes, derived as discussed below. Some selected experimental results are shown in Figs. 2–4 as projections in the ρ–T, ρ–x, and P–ρ planes together with pure-component data. As these figures demonstrate, ρ–T and P–ρ curves are almost linear (very small curvature), just as observed for

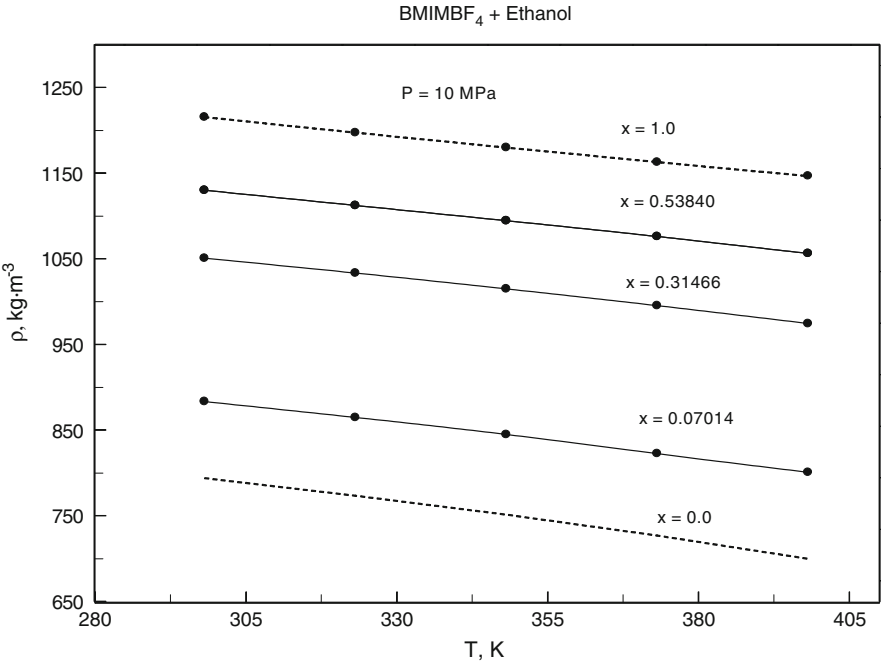

Fig. 2 Experimental densities ρ of $BMIMBF_4$ + ethanol mixtures as a function of temperature T along the various compositions and at a selected pressure of 10 MPa together with pure-component data ($x = 0.0$ for pure ethanol from Dillon and Penoncello [41] EOS)

pure-component behavior. The concentration dependence (Fig. 3) of the densities shows a considerably positive deviation from ideal behavior (up to 130–140 $kg \cdot m^{-3}$).

Figure 5a, b shows the results of the density measurements for pure $BMIMBF_4$ together with the values reported by other researchers. We made detailed comparisons of our density results for pure $BMIMBF_4$ with literature data at atmospheric and high pressures. As a result of temperature, pressure, and concentration differences between the reported data, we sometimes used an interpolating procedure (analytical method) to compare the present density data with values reported by other authors. The uncertainty of the interpolating procedure is negligibly small since the experimental ρ–T and P–ρ curves are almost linear and can be reproduced analytically with high accuracy. As one can see from Fig. 5a (A), all the available density data sets reported by various authors at atmospheric pressure for $BMIMBF_4$ fall in a range within $\pm 1.1\%$ in comparison with the present results. This figure does not include the data by Suarez et al. [17] which deviate from all the other reported data by 2%. A majority of the reported data show systematic deviations with the other data.

Two possible reasons for the large discrepancies among the various data sources are as follows: purity of the IL samples (basically water content, see below) and incorrect calibration of the instrument. A comparison of the present density data for $BMIMBF_4$ with reported data are presented in Table 2, together with the method of measurements and water content in the samples as claimed by the authors. Our data

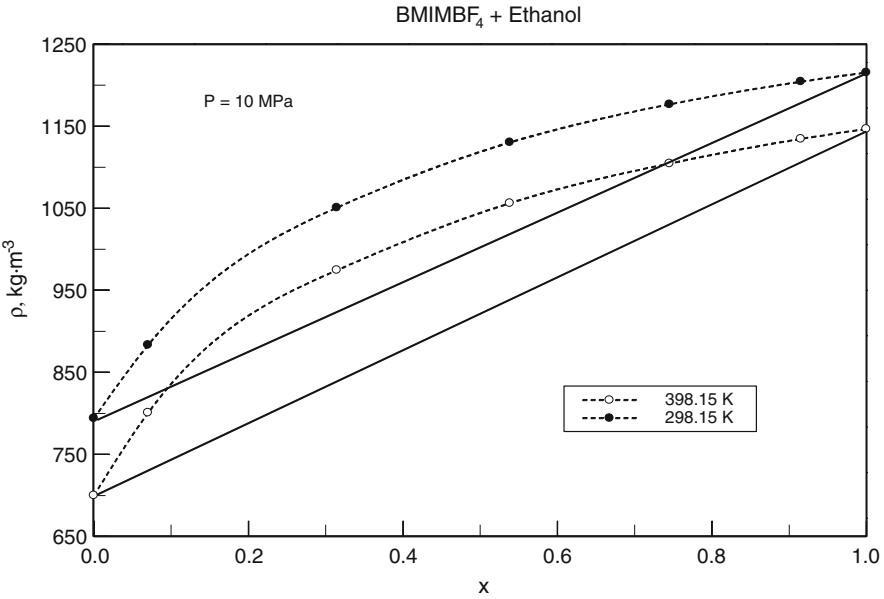

Fig. 3 Experimental densities ρ of $BMIMBF_4$ + ethanol mixtures as a function of composition x along two selected isotherms of 298.15 K and 398.15 K and a selected isobar of 10 MPa. The dashed curves guide the eye. The solid lines are an ideal mixture

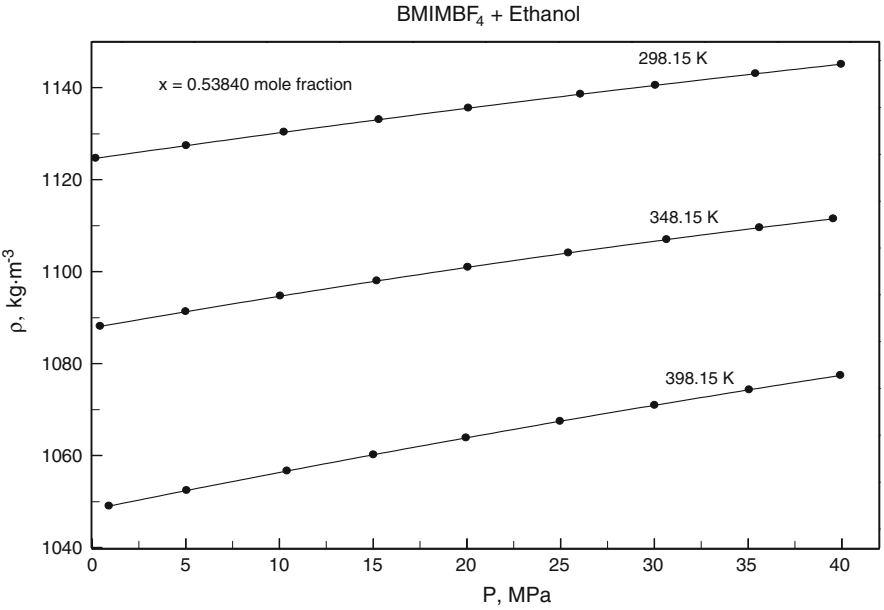

Fig. 4 Experimental densities ρ of $BMIMBF_4$ + ethanol mixtures as a function of pressure P along the selected isotherms and at a selected constant concentration of 0.5384 mole fraction of $BMIMBF_4$

Table 1 Experimental values of density, pressure, apparent molar volume, temperature, and concentration of $BMIMBF_4$ + ethanol mixtures

P (MPa)	ρ (kg·m^{-3})	ϕ_V (cm^3·mol^{-1})	P (MPa)	ρ (kg·m^{-3})	ϕ_V (cm^3·mol^{-1})	P (MPa)	ρ (kg·m^{-3})	ϕ_V (cm^3·mol^{-1})
$x = 0.0$ (Pure ethanol)[a]			$x = 0.0701$			$x = 0.3147$		
$T = 298.15$ K								
0.101	785.47	–	0.390	875.91	178.03	0.340	1044.49	184.76
5	789.79	–	5.500	880.04	177.96	5.630	1048.05	184.45
10	793.98	–	11.37	884.58	177.81	10.91	1051.47	184.14
15	797.97	–	15.13	887.37	177.71	15.28	1054.20	183.88
20	801.79	–	21.07	891.60	177.53	20.54	1057.36	183.58
25	805.45	–	25.57	894.66	177.41	25.47	1060.21	183.31
30	808.96	–	30.62	897.94	177.31	31.12	1063.34	183.01
35	812.35	–	35.86	901.17	177.25	35.80	1065.82	182.78
40	815.62	–	39.34	903.23	177.23	39.77	1067.84	182.58
$T = 323.15$ K								
0.101	763.61	–	0.290	856.52	177.35	0.340	1026.83	186.49
5	768.64	–	5.410	861.09	177.61	5.010	1030.15	186.28
10	773.47	–	10.73	865.61	177.77	10.11	1033.63	186.04
15	778.04	–	15.43	869.40	177.88	15.41	1037.07	185.80
20	782.37	–	20.33	873.16	177.98	20.75	1040.38	185.56
25	786.51	–	25.38	876.83	178.09	26.29	1043.62	185.32
30	790.46	–	30.33	880.21	178.25	30.64	1046.04	185.15
35	794.24	–	34.74	883.06	178.44	35.26	1048.48	184.97
40	797.88	–	40.01	886.25	178.64	40.12	1050.91	184.81
$T = 348.15$ K								
0.18	739.72	–	0.520	835.75	176.18	0.230	1007.50	188.33
5	745.70	–	5.340	840.67	176.77	5.740	1011.89	188.13
10	751.37	–	11.71	846.75	177.38	11.42	1016.16	187.91
15	756.67	–	15.84	850.45	177.69	15.74	1019.22	187.74
20	761.67	–	20.55	854.43	178.05	21.63	1023.15	187.52
25	766.39	–	25.38	858.25	178.43	26.12	1025.95	187.36
30	770.87	–	30.22	861.80	178.88	30.55	1028.55	187.23
35	775.14	–	35.17	865.16	179.42	35.63	1031.33	187.09
40	779.22	–	40.03	868.18	180.02	40.01	1033.56	187.00

Table 1 continued

P (MPa)	ρ (kg·m^{-3})	ϕ_V (cm^3·mol^{-1})	P (MPa)	ρ (kg·m^{-3})	ϕ_V (cm^3·mol^{-1})	P (MPa)	ρ (kg·m^{-3})	ϕ_V (cm^3·mol^{-1})
$T = 373.15$ K								
0.39	713.14	–	0.510	812.28	174.28	0.810	987.83	189.87
5	720.25	–	5.790	818.18	176.07	5.820	992.08	189.89
10	727.05	–	11.04	823.77	177.31	10.95	996.25	189.82
15	733.34	–	15.13	827.92	178.04	15.73	999.95	189.73
20	739.18	–	21.22	833.79	178.86	19.86	1003.02	189.61
25	744.65	–	25.13	837.37	179.27	25.99	1007.35	189.43
30	749.80	–	30.26	841.81	179.76	30.67	1010.47	189.29
35	754.67	–	35.52	846.10	180.23	35.22	1013.34	189.15
40	759.30	–	39.84	849.40	180.57	39.82	1016.10	189.02
$T = 398.15$ K								
0.76	683.03	–	1.010	788.85	167.92	0.960	966.26	191.06
5	691.50	–	5.750	795.42	170.47	6.350	971.33	191.39
10	699.93	–	10.15	801.14	172.20	10.93	975.46	191.52
15	707.55	–	15.11	807.16	173.70	15.62	979.51	191.56
20	714.52	–	20.74	813.42	175.13	20.15	983.26	191.54
25	720.97	–	25.13	817.89	176.16	25.17	987.21	191.47
30	726.97	–	30.85	823.16	177.55	30.41	991.12	191.36
35	732.59	–	35.86	827.28	178.86	35.16	994.46	191.25
40	737.88	–	39.99	830.32	179.98	39.85	997.59	191.14
$x = 0.5384$			$x = 0.7452$			$x = 0.9152$		
$T = 298.15$ K								
0.210	1124.67	185.82	0.180	1171.71	186.30	0.120	1199.70	186.53
5.040	1127.45	185.50	4.960	1174.16	185.97	5.140	1202.06	186.18
10.26	1130.36	185.17	10.06	1176.71	185.63	10.03	1204.31	185.85
15.32	1133.10	184.86	15.21	1179.21	185.30	15.62	1206.82	185.48
20.09	1135.59	184.57	20.36	1181.64	184.98	20.48	1208.95	185.17
26.07	1138.61	184.21	25.41	1183.95	184.67	26.14	1211.36	184.82
30.07	1140.56	183.98	30.09	1186.03	184.39	29.87	1212.91	184.59
35.41	1143.07	183.69	35.48	1188.36	184.08	35.74	1215.30	184.25
39.98	1145.14	183.45	39.92	1190.22	183.82	39.98	1216.97	184.01

Table 1 continued

P (MPa)	ρ (kg·m^{-3})	ϕ_V (cm^3·mol^{-1})	P (MPa)	ρ (kg·m^{-3})	ϕ_V (cm^3·mol^{-1})	P (MPa)	ρ (kg·m^{-3})	ϕ_V (cm^3·mol^{-1})
$T = 323.15$ K								
0.850	1106.94	188.20	0.420	1153.47	188.99	0.510	1181.35	189.36
4.890	1109.43	187.94	5.060	1156.05	188.65	4.870	1183.60	189.02
9.860	1112.40	187.62	10.74	1159.11	188.25	10.08	1186.23	188.62
14.87	1115.29	187.31	15.08	1161.39	187.94	15.21	1188.77	188.24
20.16	1118.22	186.98	20.31	1164.06	187.58	20.47	1191.31	187.86
25.84	1121.23	186.64	25.12	1166.45	187.25	25.01	1193.45	187.54
30.26	1123.49	186.39	30.08	1168.84	186.93	30.07	1195.79	187.19
35.42	1126.01	186.10	35.07	1171.16	186.62	34.96	1198.00	186.86
40.02	1128.17	185.85	40.01	1173.40	186.31	40.00	1200.22	186.53
$T = 348.15$ K								
0.450	1088.13	190.66	0.380	1134.96	191.75	0.460	1163.17	192.22
5.010	1091.32	190.34	5.360	1138.08	191.34	5.040	1165.81	191.82
10.06	1094.71	189.99	10.09	1140.95	190.95	11.21	1169.27	191.29
15.21	1098.01	189.64	15.42	1144.07	190.53	15.08	1171.38	190.96
20.06	1100.98	189.32	20.08	1146.71	190.17	20.74	1174.39	190.50
25.43	1104.11	188.98	25.41	1149.62	189.77	25.14	1176.67	190.15
30.67	1107.00	188.66	30.07	1152.07	189.43	29.98	1179.10	189.78
35.62	1109.59	188.38	35.14	1154.63	189.08	35.07	1181.59	189.40
39.56	1111.54	188.17	39.94	1156.96	188.76	39.74	1183.80	189.06
$T = 373.15$ K								
0.750	1069.65	192.92	0.520	1117.10	194.36	0.780	1145.53	195.06
5.060	1072.77	192.68	5.090	1120.20	193.97	5.140	1148.26	194.64
10.07	1076.30	192.39	10.61	1123.82	193.50	10.57	1151.58	194.12
15.34	1079.90	192.05	15.84	1127.11	193.06	15.08	1154.27	193.70
20.61	1083.37	191.71	20.09	1129.70	192.72	20.54	1157.45	193.20
25.93	1086.76	191.36	25.46	1132.84	192.29	24.67	1159.79	192.83
30.01	1089.27	191.09	30.07	1135.43	191.94	29.76	1162.61	192.39
35.03	1092.26	190.76	35.18	1138.19	191.56	36.74	1166.35	191.82
39.94	1095.08	190.45	39.92	1140.63	191.22	39.87	1167.99	191.55

Table 1 continued

P (MPa)	ρ (kg·m^{-3})	ϕ_V (cm^3·mol^{-1})	P (MPa)	ρ (kg·m^{-3})	ϕ_V (cm^3·mol^{-1})	P (MPa)	ρ (kg·m^{-3})	ϕ_V (cm^3·mol^{-1})
$T = 398.15$ K								
0.920	1049.06	195.35	0.940	1098.62	197.05	0.860	1128.45	197.84
5.060	1052.44	195.19	5.120	1101.74	196.68	5.840	1131.83	197.31
10.42	1056.68	194.91	10.07	1105.35	196.24	9.630	1134.36	196.92
15.03	1060.22	194.63	15.08	1108.88	195.78	16.47	1138.81	196.21
19.97	1063.89	194.30	20.64	1112.68	195.28	20.04	1141.07	195.85
24.98	1067.49	193.95	25.37	1115.80	194.85	25.12	1144.22	195.35
30.03	1070.98	193.60	30.28	1118.94	194.42	30.45	1147.45	194.84
35.07	1074.35	193.24	35.14	1121.93	194.01	35.74	1150.56	194.34
39.94	1077.48	192.90	39.92	1124.78	193.61	39.86	1152.93	193.96

P (MPa)	ρ (kg·m^{-3})	P(MPa)	ρ (kg·m^{-3})	P(MPa)	ρ (kg·m^{-3})
$x =$ 1.0 (BMIM BF_4)					
$T = 298.15$ K		$T = 323.15$ K		$T = 348.15$ K	
0.28	1211.19	0.73	1192.89	0.21	1174.44
5.64	1213.63	5.64	1195.30	5.96	1177.75
10.62	1215.85	10.61	1197.71	10.48	1180.30
15.34	1217.77	15.44	1200.01	15.43	1182.72
20.64	1220.29	20.46	1202.37	20.87	1185.63
25.27	1222.18	25.36	1204.64	25.85	1188.16
30.05	1223.93	30.74	1207.09	30.11	1190.19
35.41	1226.07	35.65	1209.29	35.11	1192.88
39.61	1227.81	39.85	1211.14	39.61	1194.77
T= 373.15 K		T= 398.15 K		–	
0.47	1157.24	0.87	1141.05	–	–
5.35	1160.25	6.67	1144.53	–	–
10.08	1163.09	10.49	1147.07	–	–
15.71	1166.39	15.73	1150.32	–	–
20.97	1169.38	20.98	1153.78	–	–
25.82	1172.07	25.14	1156.30	–	–

Table 1 continued

P (MPa)	ρ (kg·m^{-3})	P(MPa)	ρ (kg·m^{-3})	P(MPa)	ρ (kg·m^{-3})
30.12	1174.39	30.89	1159.52	–	–
35.53	1177.22	35.81	1162.40	–	–
39.82	1179.41	39.56	1164.38	–	–

[a] Dillon and Penoncello EOS [41]

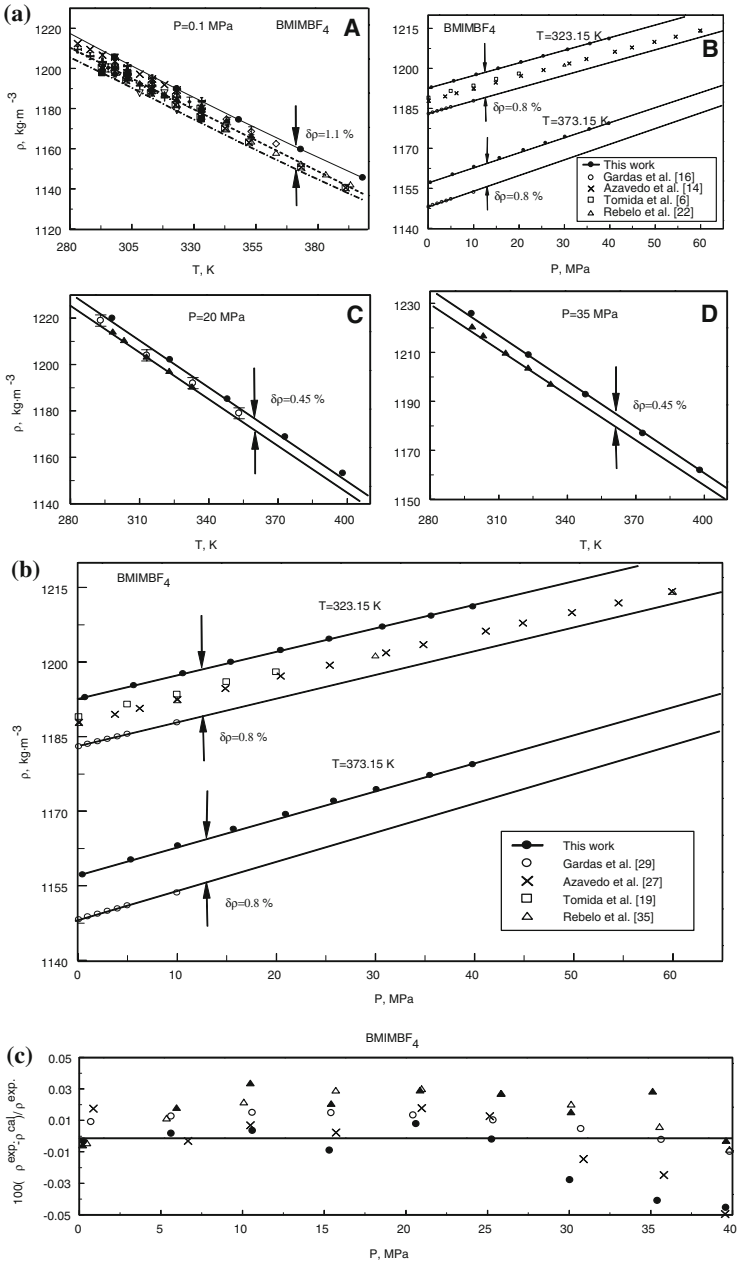

Fig. 5 (**a**, **b**) Comparison of the present results for the density of pure $BMIMBF_4$ with the data reported by other authors in the literature for four selected isobars. A: •, this work; ○, [6]; ■, [11]; □, [14]; Δ, [16]; ×, [7]; ▲, [15]; ♦, [12]; ▼, [11]; ∇, [20]; ◊, [4]; ✠, [22]; +, [23]; ⁎, [27]; ⊗, [3]; (— — ——), [13]; (·····), [25]; (— — ——), Eq. (4). B–D: •, this work; ◯, [6]; Δ, [16]; ▲, [14]. (**c**) Percentage deviations $\delta\rho = 100\left(\frac{\rho^{\exp} - \rho^{\mathrm{cal}}}{\rho^{\exp}}\right)$ of the present experimental densities for pure $BMIMBF_4$ from the values calculated with the EOS (Eq. 2): •, 298.15 K; ◯, 323.15 K; ▲, 348.15 K; Δ, 373.15 K; ×, 398.15 K

Table 2 Average absolute (AAD) and maximum (MaxDev) deviations between the present and reported data for $BMIMBF_4$[a]

Reference	AAD (%)	MaxDev (%)	Water content (ppm)	Method of density measurements
Yang et al. [8]	0.18	0.29	n.a.	PC
Gardas et al. [16]	0.76	0.82	485	VTD
Zhou et al. [15]	0.62	0.85	200	PC
de Azevedo et al. [14]	0.44	0.50	75 ± 10	VTD
Van Valkenburg et al. [38]	0.90	1.08	9600	DE40
Fredlake et al. [12]	0.46	0.69	1900	PC
Tomida et al. [6]	0.29	0.33	336 ± 100	GP
Tokuda et al. [13]	0.67	0.83	40	DGM
Kim et al. [20]	0.84	1.13	n.a.	PC
Wang et al. [11]	0.01	0.01	1600	VTD
Seddon et al. [21]	0.38	0.60	307	CDB
Zafarani-Moattar and Shekaari [23]	0.77	0.80	n.a.	VTD
Rebelo et al. [22]	0.07	0.12	75 ± 10	VTD
Sanmamed et al. [25]	0.70	0.75	1768	VTD
Lopes et al. [27]	0.45	0.53	70	VTD
Jacquemin et al. [3]	0.88	1.00	70	VTD
This work	0.00	0.00	62	VTD

[a] n.a.: no water content is reported; VTD: Vibrating-tube densimeter; PC: Pycnometer; GP: Glass piezometer; DGM: Density gravity meter; DE40: Densimeter (DE40); CDB: calibrated 10 cm^3 density bottles

are basically higher than all of the reported data by about 0.45%. As Fig. 5a (B-D), 5b shows, at high pressures (up to 35 MPa), the deviations between the present and the reported data are within 0.45–0.80%. The present results deviate by 0.76% with the data reported by Gardas et al. [16], while the data by de Azevedo et al. [14] and Tomida et al. [6] agree within 0.46 and 0.33%, respectively. This is acceptable because the effect of a small amount of water (see next section) in ILs dramatically changes the density of the IL ($BMIMBF_4$) sample. In general, the agreement between different data sets is satisfactory. This acceptable agreement between the present and the reported data demonstrates the reliability and high accuracy of the measurements for $BMIMBF_4$ + ethanol mixtures.

3.1 Equation of State

The present measured mixture densities were accurately represented by a simple Tait-type equation of state which was applied previously for pure fluids [16,31–35]:

$$\frac{\rho - \rho_0}{\rho_0} = c \log\left(\frac{B + P}{B + P_0}\right), \tag{2}$$

where parameter c is a function of concentration and almost independent of temperature or a weak function of temperature, $B(T)$ is a function of temperature only, and ρ_0 is the density of the mixture at a reference pressure $P_0 (P_0 = 0.1\,\text{MPa})$,

$$\rho_0(T, x, P = 0.1) = x\rho_1\,(T, x = 1, P = 0.1) + (1 - x)\,\rho_2\,(T, x = 0, P = 0.1) + x\,(1 - x)\Big[A_1 + (1 - 2x)\,A_2 + (1 - 2x)^2\,A_3 + (1 - 2x)^4\,A_4\Big], \quad (3)$$

where $A_1 = 473.5212$, $A_2 = 255.3281$, $A_3 = 239.7849$, and $A_4 = 197.9015$, and $\rho_1(T, x = 1, P = 0.1)$ and $\rho_2(T, x = 0, P = 0.1)$ is the density of the pure-component $BMIMBF_4$ and ethanol, respectively, at atmospheric pressure:

$$\rho_1(T, x = 1, P = 0.1) = 1483.896 - 1.06968T + 5.1949 \times 10^{-4}T^2 \text{ and} \quad (4)$$

$$\rho_2(T, x = 0, P = 0.1) = 884.060 + 0.16894T - 1.16761 \times 10^{-3}T^2. \quad (5)$$

In the present work we applied Eq. 2 to the $BMIMBF_4$ + ethanol mixture. Various versions of Eq. 2 were examined:

1. $c = c_1 + c_2x$ and $B = b_0 + b_1T + b_2T^2$, where c_i and b_i are adjustable parameters,
2. $c = xc_1 + (1 - x)c_2 + (1 - 2x)c_{12}$ and $B = b_0 + b_1T + b_2T^2$, where c_{12} and b_i are adjustable parameters, and c_1 and c_2 are the values of the c coefficient in Eq. 2 for the pure components;
3. $c = xc_1 + (1 - x)c_2 + (1 - 2x)c_{12}$ and $B = xB_1 + (1 - x)B_2 + (1 - 2x)B_{12}$, where only c_{12} and B_{12} are adjustable parameters, and (c_1, c_2) and (B_1, B_2) are the values of c and B coefficients in Eq. 2 for the pure components, respectively.

The average absolute deviations of the various versions of Eq. 2 are: $AAD = 0.246\%$, $AAD = 0.250\%$, and $AAD = 0.329\%$, respectively. The deviations for the pure-component data for ethanol and $BMIMBF_4$ are: $AAD = 0.15\%$ and $AAD = 0.016\%$, respectively. The derived values of the coefficients c_i and b_i for Version 1 of Eq. 2 for $BMIMBF_4$ + ethanol mixture are given in Table 3. In total, Eq. 2 contains a minimum of five adjustable coefficients for the mixture. This equation is valid in the temperature range from 298 K to 398 K, at pressures up to 40 MPa, and at concentrations from 0 mole to 1 mole fraction. Equation 2 represents the present densities for $BMIMBF_4$ + ethanol mixtures with an AAD of 0.246% over the whole concentration range. Figures 5c and 6 show deviation plots (percentage relative deviations) between the present measured densities and those calculated with Eq. 2 for the pure IL ($BMIMBF_4$) and $BMIMBF_4$ + ethanol mixtures. Equation 2 was used to calculate some of the derived thermodynamic and structural properties of the $BMIMBF_4$ + ethanol system, such as partial molar volumes (see below).

Table 3 Parameters b_i and c_i of Eq. 2

i	b_i	c_i
	Ethanol + $BMIMBF_4$	
0	1007.6281	–
1	−0.424866	0.3841572
2	−0.003875	−0.2650716

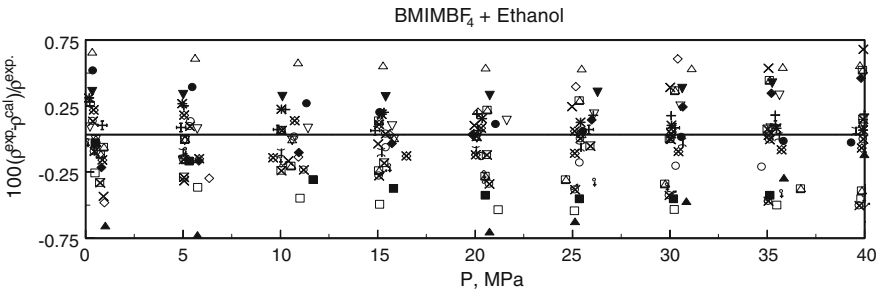

Fig. 6 Percentage deviations $\delta\rho = 100\left(\frac{\rho^{\exp} - \rho^{\mathrm{cal}}}{\rho^{\exp}}\right)$ of the present experimental densities for the BMIMBF$_4$ + ethanol mixtures from the values calculated with the EOS (Eq. 2): $x = 0.0701$, •, 298.15 K; ◯, 323.15 K; ■, 348.15 K; □, 373.15 K; ▲, 398.15 K; $x = 0.3147$, ◇, 398.15 K; ♦, 373.15 K; ∇, 348.15 K; ▼, 323.15 K; △, 298.15 K; $x = 0.5384$, +, 298.15 K; ✠, 323.15 K; ✡, 348.15 K; ☒, 373.15 K; ×, 398.15 K; $x = 0.7452$, ✱, 298.15 K; ⌗, 323.15 K; ⊗, 348.15 K; ⌖, 373.15 K; ⛥, 398.15 K; $x = 0.9152$, ⍜, 298.15; ⍝, 323.15 K; ¤, 348.15 K; ☼, 373.15 K; ↥, 398.15 K

3.2 Effect of Water Content on the Density of ILs (BMIMBF$_4$)

IL samples usually contain impurities such as Cl^- and water, which significantly change their thermophysical properties [4,25,36]. This is one of the reasons for large (within ±1.1%) scatter (see Fig. 5a, b) for the reported density data for BMIMBF$_4$. The effect of impurities (especially water content) in the IL sample on their measured properties has been widely discussed in the literature (see, for example, [3,10,25,36,37]). It is very difficult to keep water out of ILs. Molecular dynamic simulations and spectroscopic studies [39] indicate strong interactions between water molecules and the anions of the ILs are present. Dominguez-Vidal et al. [39] found stretching of the H-bonds between water and the BF_4^- anions. Therefore, it is very hard to completely remove the water from the ILs by using conventional techniques.

In order to estimate the effect of water content on the density of BMIMBF$_4$, we can expand the density of the impure (dilute impure) sample as a series of powers of the concentration x (near $x = 0$, absolute pure sample), taking only the first terms of the expansion,

$$\rho(x, T_0, P_0) = \rho(x = 0, T_0, P_0) + \left(\frac{\partial \rho}{\partial x}\right)_{T_0 P_0, x=0} x + \left(\frac{\partial^2 \rho}{\partial x^2}\right)_{T_0 P_0, x=0} x^2 + \cdots, \tag{6}$$

where $\rho(x = 0, T_0, P_0)$ is the density of the "ideal" sample (absolute pure sample) at a given T_0 and P_0; $\rho(x, T_0, P_0)$ is the density of the real sample (impure, water content sample) at a given T_0 and P_0; and x is the impurity concentration (water content). As one can see from Eq. 6, as a first approximation, the values of the density of the real sample depend on the derivative $(\partial\rho/\partial x)_{T_0 P_0, x=0}$, i.e., the initial slope of the concentration dependences of the density ρ of dilute ($x \to 0$) BMIMBF$_4$ + water mixtures at a fixed T_0 and P_0. The sign of $(\partial\rho/\partial x)_{T_0 P_0, x=0}$ depends on the nature

of the impurity. For water, $(\partial\rho/\partial x)_{T_0 P_0, x=0}$ is negative; therefore, small amounts of water in $BMIMBF_4$ decrease the density of the IL sample. The derived values [15,22] of the derivative $(\partial\rho/\partial x)_{T_0 P_0, x=0}$ at $T_0 = 298.15$ and 323.15 K and at $P_0 = 0.1$ MPa are $-1827.7\,\mathrm{kg\cdot m^{-3}}$ and $-1336.0\,\mathrm{kg\cdot m^{-3}}$, respectively. These values of $(\partial\rho/\partial x)_{T_0 P_0, x=0}$ were used to quantitatively estimate the effect of small impurities (water content) on the measured densities of $BMIMBF_4$. For example, the values of the density of $BMIMBF_4$ due to a dilute impurity effect ($x = 0.001$ mole fraction of water or about 79 ppm) calculated with Eq. 6 at temperatures of 298.15 K and 323.15 K decrease by $1.83\,\mathrm{kg\cdot m^{-3}}$ (or 0.21%) and $1.34\,\mathrm{kg\cdot m^{-3}}$ (or 0.16%), respectively. Therefore, small amounts of water ($x = 0.001$ mole fraction) can cause an uncertainty in the density of approximately 0.2%.

Usually (see Table 2), a typical sample of $BMIMBF_4$ used by various authors contains 75–1,900 ppm (or 0.001–0.023 mole fraction) of water. Therefore, the effect of water content on the density of $BMIMBF_4$ reported by these authors is within $8\,\mathrm{kg\cdot m^{-3}}$ to $11\,\mathrm{kg\cdot m^{-3}}$ or 0.7–0.9%. Approximately the same level of deviations was found between the present density data and the data reported by other authors [16,20,23,25,38]. As Table 2 shows, the density measured by Gardas et al. [16] is lower than the present results by 0.76%, while the values of density reported by Zhou et al. [15] deviate by 0.62%. The water content in the sample used by Zhou et al. [15] is about 200 ppm. According to Eq. 6, the effect of water content on the measured densities is about 0.38–0.51% which is close to 0.62%. The data by Azevedo et al. [14] differ from the present density data by 0.44%, and the water content is about 75 ppm. This amount of water content in the $BMIMBF_4$ sample corresponds to a density change of 0.25%; therefore, the agreement between our data and the values reported by Azevedo et al. [14] is within 0.19%. The same amount (0.001 mole fraction) of water and dichloromethane causes different changes in the density. Dichloromethane (0.001 mole fraction, $(\partial\rho/\partial x)_{T_0 P_0, x=0} = 44.19\,\mathrm{kg\cdot m^{-3}}$ at 298.15 K and 0.1 MPa) increases the density of $BMIMBF_4$ by about $0.044\,\mathrm{kg\cdot m^{-3}}$ (about 0.004%), while the same amount of water content in $BMIMBF_4$ at the same T and P decreases the density by $1.83\,\mathrm{kg\cdot m^{-3}}$ (0.21%).

The derivative $(\partial\rho/\partial x)_{T_0 P_0, x=0}$, which determines the magnitude of the effect of impurity on the density in the infinite dilution limit (for small impurities, $x \to 0$), can be expressed as

$$\lim_{X\to 0}\left(\frac{\partial\rho}{\partial x}\right)_{PT} = (\rho K_T)\lim_{X\to 0}\left(\frac{\partial P}{\partial x}\right)_{VT} = \rho K_T\left(\frac{\partial P}{\partial x}\right)^{\infty}_{TV} \tag{7}$$

where $\left(\frac{\partial P}{\partial x}\right)^{\infty}_{TV}$ is the initial slope ($x \to 0$) of the P–x curve, the isotherm-isochore Krichevskii function [40]; and ρ and K_T are the density and compressibility of the pure solvent (in our case, an IL). Thus, using Eq. 7, Eq. 6 can be rewritten in a simple form as

$$\Delta\rho = K_T\left(\frac{\partial P}{\partial x}\right)^{\infty}_{TV} x, \tag{8}$$

where $\Delta\rho = [\rho\,(x, T_0, P_0) - \rho\,(x = 0, T_0, P_0)]/\rho\,(x = 0, T_0, P_0)$ is the relative deviation of the measured density of an impure sample from an ideally pure sample or the magnitude of the effect of the impurity on the measured values of the density. As one can see, the values of $\Delta\rho$ are defined only by the isothermal compressibility K_T of the pure sample and the sign and magnitude of the Krichevskii function $\left(\frac{\partial P}{\partial x}\right)_{TV}^{\infty}$. As will be shown below (see Sect. 3.5),

$$K_T \left(\frac{\partial P}{\partial x}\right)_{TV}^{\infty} = \overline{V}_2^0/V - 1 \text{ or } \left(\frac{\partial \rho}{\partial x}\right)_{PT} = \rho^2 \left(\overline{V}_2^0 - V\right). \tag{9}$$

Thus, the impurity effect on the density is defined as

$$\Delta\rho = \rho \left(\overline{V}_2^0 - V\right) x \text{ or } \Delta\rho = \left(\overline{V}_2^0/V - 1\right) x. \tag{10}$$

Therefore, the impurity effect on the density depends on the Krichevskii function $(\partial P/\partial x)_{TV}^{\infty}$ or on the ratio of the partial molar volume at infinite dilution $\overline{V}_2^0$ and the molar volume V of the pure solvent, $\left(\overline{V}_2^0/V\right)$.

3.3 Excess Molar Volume

The excess molar volumes for the $BMIMBF_4$ + ethanol mixtures were calculated using the present molar volume data for the mixtures and pure-component values calculated from Dillon and Penoncello [41] for pure ethanol and the present data for pure $BMIMBF_4$ (see Table 1) with the following relation:

$$V_{\mathrm{m}}^{\mathrm{E}}(P, T, x) = V_{\mathrm{m}}(P, T, x) - xV_{\mathrm{m}}(P, T, 1) - (1 - x)V_{\mathrm{m}}(P, T, 0), \tag{11}$$

where x is the mole fraction of $BMIMBF_4$, $V_{\mathrm{m}}(P, T, x)$ is the experimentally determined molar volume of the mixture of concentration x at temperature T and pressure P, and $V_1 = V_{\mathrm{m}}(P, T, 1)$ and $V_2 = V_{\mathrm{m}}(P, T, 0)$ are the molar volumes of the pure components at the same pressure P and temperature T. The derived values of $V_{\mathrm{m}}^{\mathrm{E}}$ for the selected temperatures and pressures are given in Fig. 7 as a function of mole fraction x at selected temperatures and at a pressure of 10 MPa. One can note that the values of $V_{\mathrm{m}}^{\mathrm{E}}$ for the $BMIMBF_4$ + ethanol mixtures are negative for all measured temperatures and pressures over the whole composition range. The negative values of the excess molar volumes $V_{\mathrm{m}}^{\mathrm{E}}$, contributing to a contraction in volume, are dominant. Therefore, $BMIMBF_4$ + ethanol mixtures are members of a class often called "attractive" mixtures.

As one can see, the curves of excess molar volumes of $BMIMBF_4$ + ethanol mixtures are noticeably skewed toward a low mole fraction of $BMIMBF_4$. The excess molar volume minimum is found at a concentration of about 0.3 mole fraction of $BMIMBF_4$. The same trend was also found (Wang et al. [11]) in $V_{\mathrm{m}}^{\mathrm{E}}$ for ionic liquid mixtures containing organic solutes (alcohols). This can be attributed partly to the

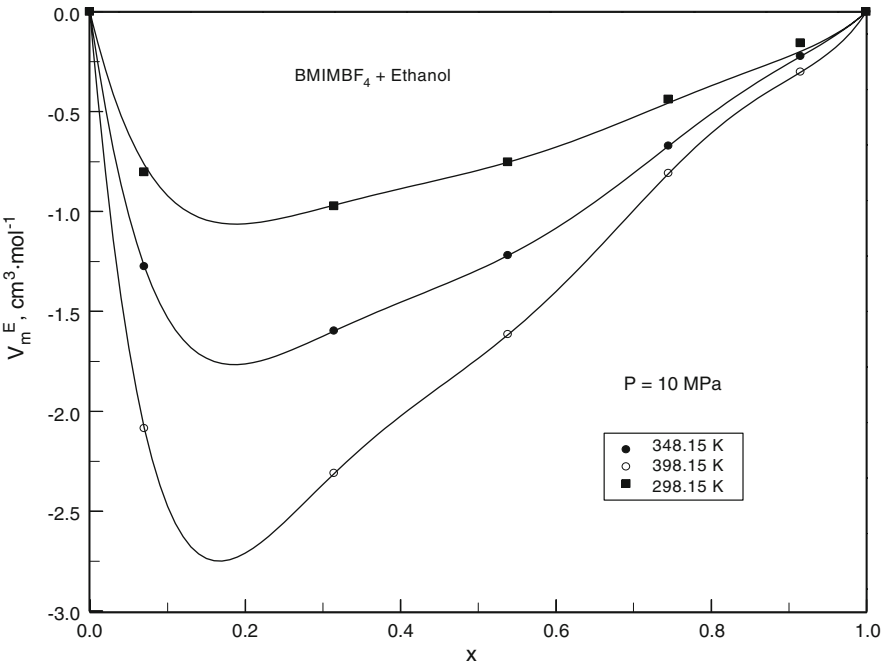

Fig. 7 Excess molar volumes V_m^E of $BMIMBF_4$ + ethanol mixtures as a function of concentration x for a selected isobar of 10 MPa and at selected temperatures

differences in the size of the ions (BF_4^-, $[BMIM]^+$) and ethanol molecules. Therefore, the chemical interactions (non-physical nature of the intermolecular interactions) between ethanol molecules and IL ions in this mixture are playing a very important role in determining the volumetric properties (excess molar properties). The addition of ethanol to $BMIMBF_4$ may result in very significant changes in the topology of ethanol or $BMIMBF_4$ since the negative excess molar volume represents a packing effect. As one can see from Fig. 7, the difference between the mixture molar volume V_{mix} and the ideal mixture molar volume $V_{id} = x V_1 + (1 - x) V_2$ is large (maximum value of about $-2.5\,cm^3 \cdot mol^{-1}$ at 298.15 K and 10 MPa). The maximum relative uncertainty, δV_m^E, in the derived values of V_m^E can be approximately estimated from the following relation (Abdulagatov and Azizov [42,43]):

$$\delta V_m^E \cong \delta V_{mix} V_{mix}/(V_{mix} - V_{id}) + \delta V_1 V_1/(V_{mix} - V_{id}) + \delta V_2 V_2/(V_{mix} - V_{id}), \tag{12}$$

where δV_{mix}, δV_1, and δV_2 are the relative uncertainties in the mixture and pure-component molar volume determinations, respectively. The uncertainty in the V_m^E calculation from Eq. 12 is within 1.7–2.7% depending on the temperature, pressure, and concentration. At concentrations close to the pure components, the uncertainty in V_m^E increases to 5–15% and more.

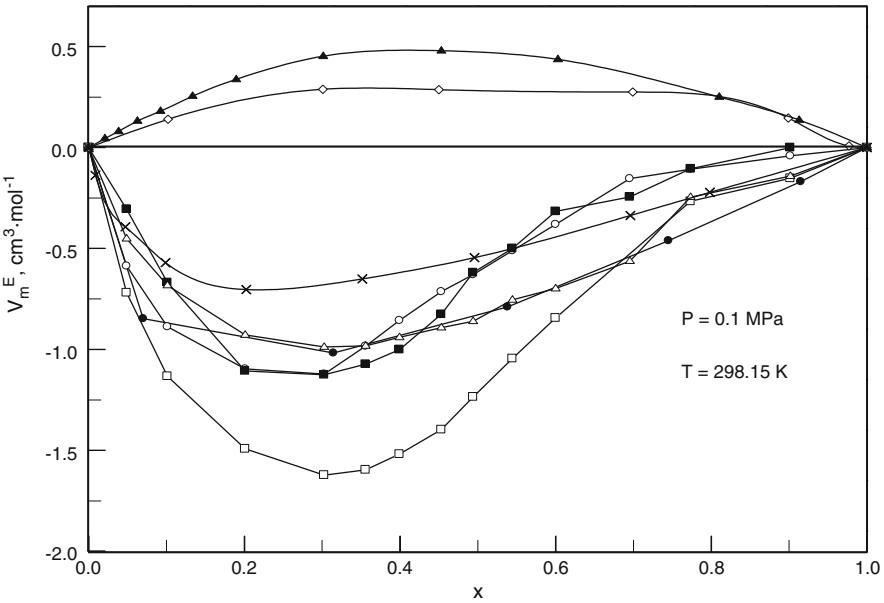

Fig. 8 Comparison of excess molar volumes V_m^E of $BMIMBF_4$-containing binary mixtures as a function of concentration x at atmospheric pressure and at selected isotherm of 298.15 K together with the present results for ethanol + $BMIMBF_4$. ●, this work ($BMIMBF_4$+ ethanol); ◯, ($BMIMBF_4$+ acetonitrile) [11]; ■, ($BMIMBF_4$+ dichlormethane) [11]; □, ($BMIMBF_4$+ 2-butanone) [11]; Δ, ($BMIMBF_4$+ N,N-dimethylformamide) [11]; ×, ($BMIMBF_4$+ methanol) [23]; ▲, ($BMIMBF_4$+ H_2O) [22]; ◇, ($BMIMBF_4$+ NTf_2) [27]

Figure 8 shows the concentration dependence of the excess molar volumes of a series of $BMIMBF_4$-containing binary mixtures with the same first component ($BMIMBF_4$) and various second components (organic solvents, other ILs, alcohol, and water) at a selected temperature of 298.15 K and at a pressure of 0.1 MPa. This figure demonstrates the effect of the nature of the second component on the values and concentration dependence behavior of the excess molar volumes of $BMIMBF_4$-containing mixtures. As one can see from Fig. 8, the introduction of alcohols and other organic solvents in the IL ($BMIMBF_4$) structure results in considerable decreases in the excess molar volumes to more negative values. The location of the maximum of V_m^E is almost always the same. The introduction of water molecules and other IL ions [NTf_2] (see Fig. 8) in the IL ($BMIMBF_4$) structure increases the excess molar volumes to positive values at the same thermodynamic (P, T, x) conditions. As Fig. 8 shows, among these binary mixtures, $BMIMBF_4$ + ethanol shows intermediate values of excess molar volumes, while 2-butanone + $BMIMBF_4$ shows lower values. The excess molar volumes for $BMIMBF_4$ + methanol mixtures are larger than those for $BMIMBF_4$ + ethanol.

3.4 Apparent Molar Volume

The values of the apparent molar volume ϕ_V are very useful tools for understanding the interactions occurring in mixtures. Studies of the apparent molar volumes of mixtures are used to examine ion-solvent, ion-ion, and solvent–solvent (structural) interactions,

i.e., to provide useful information on the nature of the interactions between dissolved ions (BF_4^-) and molecules of a solvent. In this work the apparent molar volumes ϕ_V were calculated from measured mixture densities ρ_{mix} and pure ethanol densities ρ_0 (Dillon and Penoncello [41]) by the usual relationship,

$$\phi_V = \frac{(\rho_0 - \rho_{\text{mix}})}{m\rho_{\text{mix}}\rho_0} + \frac{M}{\rho_{\text{mix}}}, \tag{13}$$

where M is the molar mass of the ILs ($BMIMBF_4$) and m is the mixture molality ($\text{mol} \cdot \text{kg}^{-1}$). We examine the behavior of the apparent molar volumes of $BMIMBF_4$ + ethanol as a function of concentration, temperature, and pressure. The derived values of ϕ_V are given in Table 1 and shown in Fig. 9 as a function of temperature at a selected pressure of 10 MPa as an example of the present results. The uncertainty of the derived values of was assessed by analyzing Eq. 13 (Abdulagatov and Azizov, [44]). The maximum relative uncertainty in the apparent molar volume determination is about 2% at low concentrations (below $2m$) and 0.7% at high concentrations (above $2m$). As Table 1 shows, the apparent molar volume ϕ_V rises rapidly at low concentrations (below $10\,\text{mol} \cdot \text{kg}^{-1}$), while at higher concentrations, ϕ_V is almost constant (weakly changes with m). Figure 9 shows that the apparent molar volume ϕ_V increases with temperature at concentrations above 0.3147 mole fraction and at constant pressures, while at low concentrations (dilute mixture) below 0.3147 mole fraction, ϕ_V decreases slightly up to a temperature of 373 K and then decreases considerably at higher temperatures. Probably at high temperatures (above 398 K), ϕ_V becomes negative as for most mixtures.

The derived apparent molar volumes ϕ_V for $BMIMBF_4$ + ethanol have been used to calculate the values of the apparent molar volume ϕ_V^0 at infinite dilution at various temperatures and pressures. In the limit of infinite dilution, the apparent molar volume of the solute $\phi_V(P, T, m \to 0)$ becomes equal to the partial molar volume ($\lim_{m\to 0} \phi_V = \phi_V^0 = \overline{V}_2^0$). Of more fundamental interest (for example, to study ion-solvent interactions), are the partial molar volumes of the ILs at infinite dilution $\overline{V}_2^0$ (where ion–ion interactions vanish). The standard procedure for calculating ϕ_V^0 or $\overline{V}_2^0$ is to extrapolate to infinite dilution ($m \to 0$), based on the extended Redlich–Mayer relation (Redlich and Mayer [45] and Roux et al. [46]):

$$\phi_V = \phi_V^0 + A_V\sqrt{m} + b_V m, \tag{14}$$

where $A_V = kw^{3/2}$ is the theoretical Debye-Hückel limiting slope for volumes, $w = 0.5\sum_i \nu_i Z_i^2$, k depends on the temperature and the physical properties [46] (dielectric constant D and compressibility β) of the solvent (pure ethanol—Dillon and Penoncello [41] and Hiejima and Yao [47]), ν_i is the number of ions of species i formed from one molecule of dissociating ILs, Z_i is the charge on species i; m is the molality, and b and d are empirical coefficients. As a rule, this relationship is applied at fixed pressure P and temperature T. The infinite-dilution values of $\phi_V(\overline{V}_2^0)$ are obtained by extrapolating Eq. 14 to zero concentration ($m \to 0$, to infinite dilution). The derived results of the partial molar volumes $\overline{V}_2^0$ for the various temperatures and three

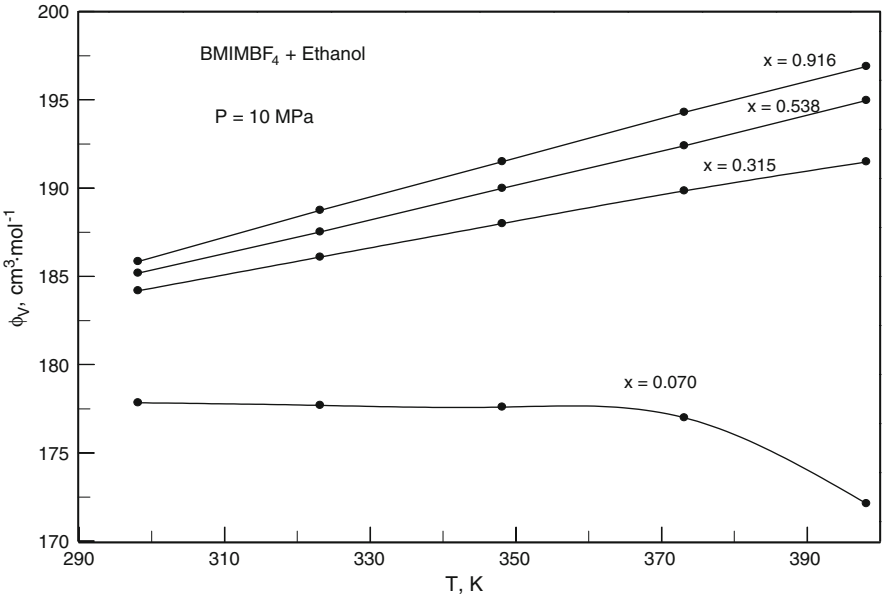

Fig. 9 Apparent molar volumes ϕ_V for $BMIMBF_4$ as a function of temperature T for a selected isobar of 10 MPa and various concentrations

selected pressures (0.1, 10, and 35 MPa) are given in Table 4 together with the values of parameters A_V and b_V in Eq. 14. As one can see from Fig. 10, at low pressures (below 35 MPa), ϕ_V^0 slightly changes almost linearly with temperature up to 373 K and then sharply decreases at high temperatures. At high pressures (above 35 MPa), ϕ_V^0 is almost independent of temperature.

3.5 Partial Molar Volume and Structural Properties of Dilute Mixtures of $BMIMBF_4$ + Ethanol

The partial molar volume at infinite dilution $\overline{V}_2^0$ is a very fundamental property of the mixture [48–50]. For example, it can be expressed as a simple integral by using the direct correlation function (DCF) [51,52] (see Eqs. 16 and 17 below). The partial molar volumes $\overline{V}_i, i = 1, 2$, are obtained from the slope of the tangent $(\partial V_m/\partial x)_{PT}$ [47–50] as

$$\overline{V}_1 = V_m - x\left(\frac{\partial V_m}{\partial x}\right)_{P,T}, \quad \overline{V}_2 = V_m + (1-x)\left(\frac{\partial V_m}{\partial x}\right)_{P,T}. \tag{15}$$

Figure 11 shows the concentration dependence of the partial molar volumes $\overline{V}_i$ calculated with Eq. 15 using the present molar volume data and Eq. 2. At infinite dilution, $\overline{V}_2^0$ can be calculated using concentration derivatives of pressure $\left(\frac{\partial P}{\partial x}\right)_{TV}^{\infty}$(Krichevskii function) [47–52] and pure solvent properties (density and isothermal compressibility).

Table 4 Parameters of Eq. 14 as a function of temperature

T (K)	ϕ_V^0 ($cm^3 \cdot mol^{-1}$)	$A_V(mol^{-1} \cdot kg)^{1/2}$	$b_V(mol^{-1} \cdot kg)$
$P = 0.1$ MPa			
298.15	176.8239	2.1884	−0.1026
323.15	175.3807	3.1198	−0.1455
348.15	173.3794	4.2046	−0.1961
373.15	170.7004	5.4066	−0.2515
398.15	162.2379	8.0612	−0.3783
$P = 10$ MPa			
298.15	176.6627	2.0711	−0.0971
323.15	175.9200	2.8385	−0.1322
348.15	175.1652	3.6030	−0.1673
373.15	174.0237	4.4595	−0.2073
398.15	167.6418	6.6366	−0.3120
$P = 35$ MPa			
298.15	176.9000	1.9424	−0.0912
323.15	176.5690	2.3143	−0.1083
348.15	176.9380	2.7963	−0.1309
373.15	177.0000	3.0481	−0.1421
398.15	176.3080	4.1182	−0.1939

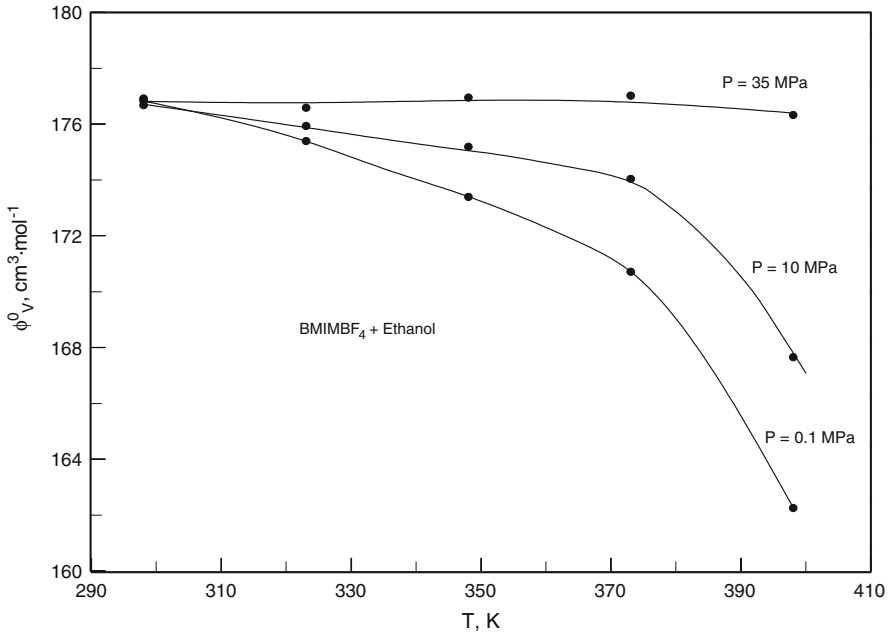

Fig. 10 Apparent molar volumes at infinite dilution ϕ_V^0 for $BMIMBF_4$ as a function of temperature T for three selected isobars of 0.1, 10, and 35 MPa

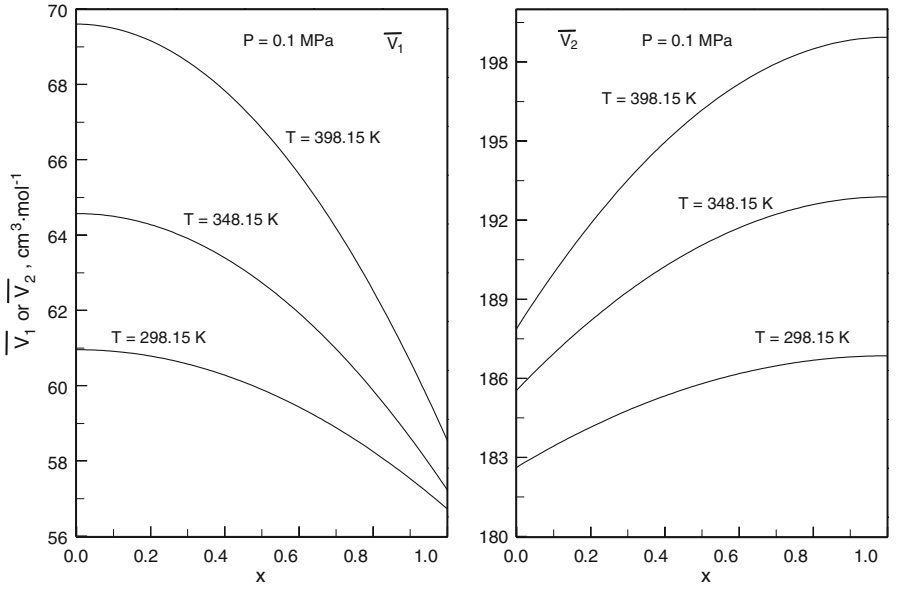

Fig. 11 Partial molar volumes $\overline{V}_i (i = 1, 2)$ for $BMIMBF_4$ as a function of concentration for three selected isotherms and at atmospheric pressure

Figure 12 demonstrates the calculated values of the Krichevskii parameter for $BMIMBF_4$ + ethanol as a function of the pure ethanol density (left) and temperature (right) for selected isotherms and isochores using Eq. 2. As this figure shows, the Krichevskii function shows very small changes with temperature, while the density dependence is considerable.

It is well known that the thermodynamic behavior of dilute mixtures depends on microscopic phenomena involving local density perturbations induced by the presence of the solute molecules. The thermodynamic behavior of dilute mixtures is extremely important for the understanding of solute and solvent molecular interactions and the microscopic structure of solutions. In general, the thermodynamic behavior of infinitely dilute mixtures can be completely characterized by the Krichevskii function which is equal to the derivative $(\partial P/\partial x)_{T_0 V_0, x=0}$ calculated at fixed temperature and volume as $x \to 0$ [53]. The Krichevskii function $J = \left(\frac{\partial P}{\partial x}\right)_{VT}^{\infty}$ has a simple physical meaning and a straightforward connection to total correlation function integrals (TCFI) [47–50,54–56]:

$$\left(\frac{\partial P}{\partial x}\right)_{TV}^{\infty} = \rho RT \frac{\rho H_{11} - \rho H_{12}}{1 + \rho H_{11}}, \tag{16}$$

where H_{11} and H_{12} are the total correlation function integrals (TCFI) defined as $H_{ij} = \int h_{ij}(r)\mathrm{d}r$; $h_{ij}(r) = g_{ij}(r) - 1$ is the total correlation function for i–j pair interactions; $g_{ij}(r)$ is the radial distribution function; and $H_{11} = (K_T RT) - \rho^{-1}$ is the TCFI for i–i pair (pure solvent molecules) interactions. In terms of the direct

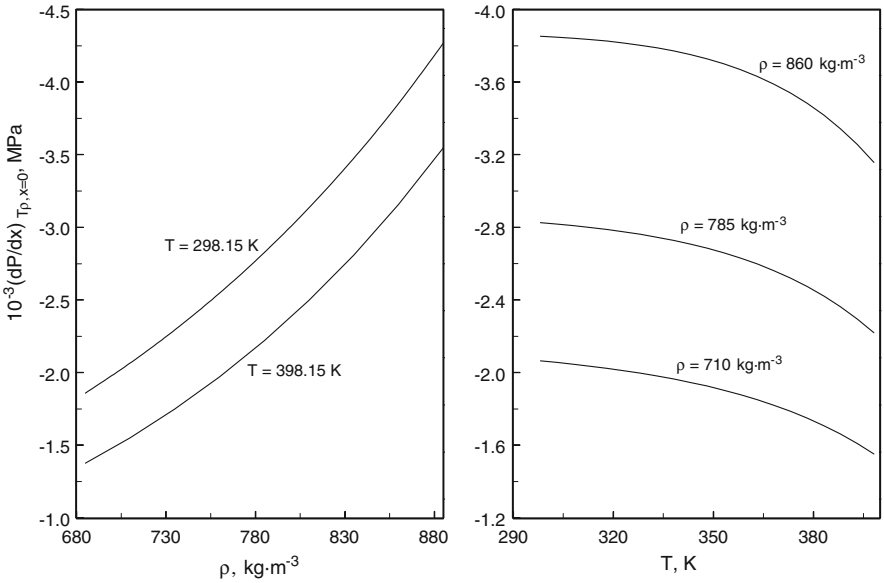

Fig. 12 Density (left) and temperature (right) dependences of the Krichevskii function for two selected temperatures of 298.15 and 398.15 K and along three isochors

correlation function (DCF) $c_{ij}(r)$ between molecules of type i and j [51,52,57–60], the Krichevskii function J is defined as

$$J = RT\rho^2(C_{11} - C_{12}), \tag{17}$$

where C_{11} and C_{12} are the direct correlation function integrals (DCFI) defined as $C_{ij} = \int c_{ij}(r)\mathrm{d}r$; $c_{ij}(r)$ is the direct correlation function for i–j pair interactions; and $(1 - \rho_1 C_{11}) = (\rho_1 K_T RT)^{-1}$ is the DCFI for i–i (pure solvent molecules) pair interactions. The DCFIs are related to the TCFI by the integrated Ornstein–Zernike equation [57]. The differences between direct (C_{11}–C_{12}) and total ($H_{11} - H_{12}$) correlation functions of solute–solvent ($BMIMBF_4$ and ethanol) and solvent–solvent (ethanol–ethanol) molecules as a function of the pure solvent (ethanol) density calculated with Eqs. 16 and 17 using the Krichevskii function are presented in Fig. 13. The comparison between C_{11} and C_{12} and H_{11} and H_{12} for a selected isotherm of 398.15 K at 0.1 MPa is shown in Fig. 14.

As one can see, the Krichevskii function is related to the DCF (17) and takes into account the effects of the intermolecular interactions between neutral molecules of solvent and solute (ILs) ions that determine the thermodynamic properties of dilute mixtures. Now it is very clear that the effect of dilute impurities on the measured thermodynamic properties (density, for example, see Sect. 3.2) strongly depend on the nature of intermolecular interactions between the pure solvent and impure molecules. The values of the Krichevskii function, $(\frac{\partial P}{\partial x})_{TV}^{\infty}$, also associated with the behavior of the microstructure of the dilute mixture (see below, Eq. 20), measures the finite microscopic rearrangement of the solvent structure around the infinitely dilute solute relative

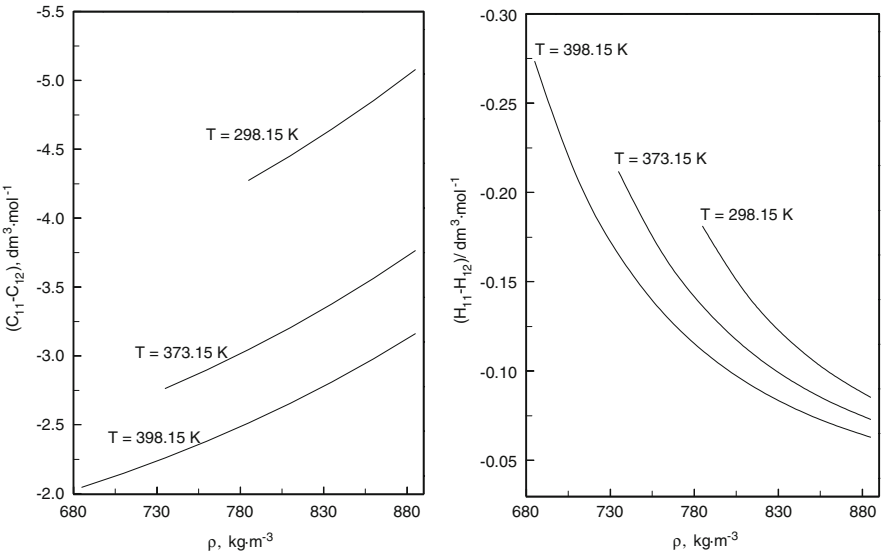

Fig. 13 Direct and total correlation integrals differences for 1–1 and 1–2 pair interactions between ethanol–ethanol molecules and ethanol-BMIMBF$_4$ (ion) as a function of density for three selected isotherms

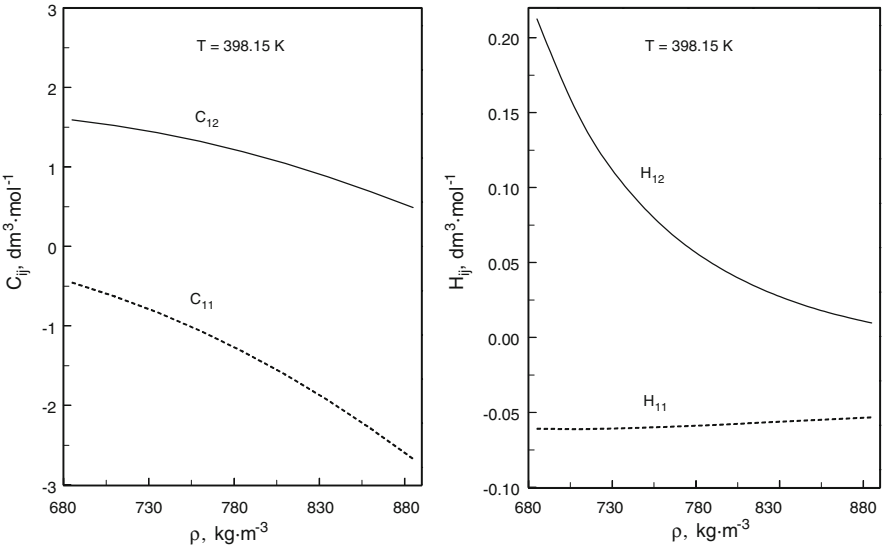

Fig. 14 Direct (C_{ij}) and total (H_{ij}) correlation integrals for 1–1 and 1–2 pair interactions between ethanol–ethanol and ethanol–IL ion as a function of density for a selected isotherm of 398.15 K

to the solvent structure ideal solution. It can be expressed by the DCFI C_{ij} for ij pair interactions by Eq. 17. The DCFI C_{12} depends only on solute–solvent interactions and is related to J by [40]

$$-C_{12} = \frac{1}{RT\rho^2}\left[J + \frac{1}{K_T}\right] - \frac{1}{\rho} \text{ or } -C_{12} = \frac{\overline{V}_2^0}{K_T RT\rho} - V. \tag{18}$$

The Krichevskii function J and C_{12} are strong functions of the density of the pure solvent ρ and weakly dependent on the temperature T. The TCFI H_{12} can also be calculated as

$$-H_{12} = -K_T J - 1 + K_T RT\rho \text{ or } -H_{12} = \overline{V}_2^0 / V. \tag{19}$$

The Krichevskii function also defines the structural properties of infinite dilute mixtures, namely, the excess number of solvent (ethanol) molecules N_{exc}^{∞} (structural parameter) around the infinitely dilute solute ($BMIMBF_4$) relative to that number around any other solvent (ethanol) molecule as [51,52]

$$N_{exc}^{\infty} = -K_T \left(\frac{\partial P}{\partial x}\right)_{TV}^{\infty}. \tag{20}$$

Figure 15 shows the density dependence of the excess number of solvent (ethanol) molecules, N_{exc}^{∞}, around the infinitely dilute solute ($BMIMBF_4$) along the various isotherms calculated from Eq. 20 using the isothermal compressibility of pure ethanol (Dillon and Penoncello [41]) and derived values of the Krichevskii function. As one can see from Fig. 15, the excess number of solvent (ethanol) molecules N_{exc}^{∞} around the IL ions in the infinite dilution limit is positive (the Krichevskii parameter is negative). This means that when exchanging a solvent (ethanol) molecule by one solute (IL) ion at constant volume and temperature, the local density of ethanol molecules around ILs ions is increasing compared with the ideal mixture or bulk density of pure ethanol (see Fig. 16). Thus, $BMIMBF_4$ + ethanol is an "attractive" mixture, $\left(\frac{\partial P}{\partial x}\right)_{TV}^{\infty} < 0$ [50,52]. It is obvious that the values of the Krichevskii function $\left(\frac{\partial P}{\partial x}\right)_{TV}^{\infty}$, associated also with the behavior of the microstructure of the dilute mixture.

4 Conclusions

The densities of five binary $BMIMBF_4$ + ethanol mixtures with compositions of (0.0701, 0.3147, 0.5384, 0.7452, and 0.9152) mole fraction $BMIMBF_4$ and of pure $BMIMBF_4$ have been measured with a vibrating-tube densimeter. Measurements were performed at temperatures from 298 K to 398 K and at pressures up to 40 MPa. The volumetric properties (excess, apparent, and partial molar volumes) were calculated as a function of temperature, pressure, and concentration using the measured densities. The values of the excess molar volume for $BMIMBF_4$ + ethanol mixtures are negative at all measured temperatures, pressures, and concentrations. The excess molar volume minimum is found at a concentration of about 0.3 mole fraction of $BMIMBF_4$. The

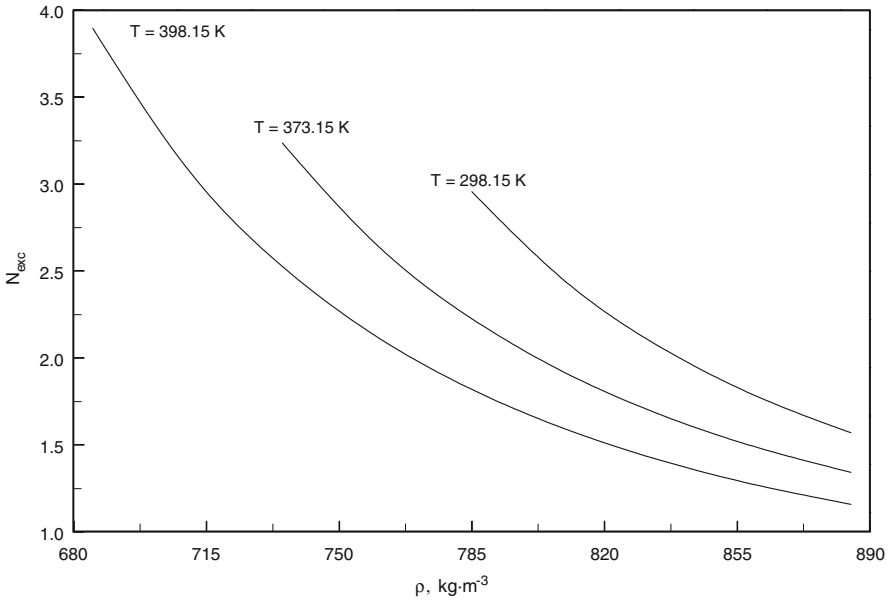

Fig. 15 Number of ethanol molecules (cluster size N_{exc}) around an IL ion in excess of that found around an ethanol molecule, as a function of density along three isotherms

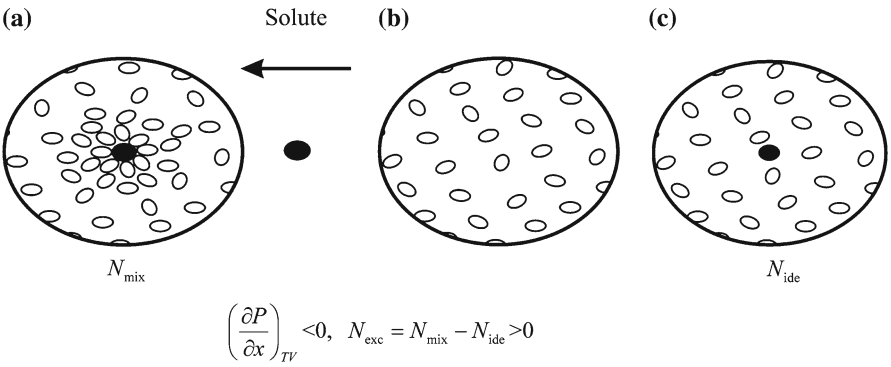

Fig. 16 Schematic representation of the local microstructure of the dilute $BMIMBF_4$ + ethanol mixture. $N_{exc} = N_{mix} - N_{ide}$, where N_{mix} is the number of ethanol molecules around IL ion in a real mixture and N_{ide} is the number of ethanol molecules around IL ion in an ideal mixture. A: infinite dilute $BMIMBF_4$ + ethanol mixture; B: pure ethanol; C: ideal $BMIMBF_4$ + ethanol mixture

Krichevskii function is calculated using the measured (P, ρ, Tx). It was found that the Krichevskii function for $BMIMBF_4$ + ethanol mixtures is negative; therefore, this mixture belongs to the "attractive" systems. The effect of water content on the measured values of density was studied using the concept of the Krichevskii function. The measured P, ρ, T, x data were used to develop a Tait–type equation of state (EOS) for

the mixture and pure components. It was shown that the parameter c in the Tait EOS is a linear function of concentration, while parameter B is a function of temperature only or almost independent of concentration (very weak function of concentration). The values of the total and direct correlation integrals and cluster size (structural properties) for dilute $BMIMBF_4$ + ethanol mixtures were calculated using the Krichevskii function.

Acknowledgments I. M. Abdulagatov thanks the Physical and Chemical Properties Division at the National Institute of Standards and Technology for the opportunity to work as a Guest Researcher at NIST during the course of this research. Dr. J.T. Safarov thanks the Alexander von Humboldt Foundation of Germany for the support of his research at the Rostock University of Germany. The authors would also like to thank Dr. J.W. Magee for his interest and useful discussions regarding the work.

References

1. J.M. Crosthwaite, S.N.V.K. Aki, E.J. Maginn, J.F. Brennecke, J. Phys. Chem. B **108**, 5113 (2004)
2. J.M. Crosthwaite, M.J. Muldoon, S.N.V.K. Aki, E.J. Maginn, J.F. Brennecke, J. Phys. Chem. B **110**, 9354 (2006)
3. J. Jacquemin, P. Husson, A.A.H. Padua, V. Majer, Green Chem. **8**, 172 (2006)
4. K.R. Seddon, A. Stark, M.-J. Torres, Pure Appl. Chem. **72**, 2275 (2000)
5. G. Annat, D.R. MacFarlane, M. Forsyth, J. Phys. Chem. B **111**, 9018 (2007)
6. D. Tomida, A. Kumagai, K. Qiao, C. Yokoyama, Int. J. Thermophys. **27**, 39 (2006)
7. Q.-G. Zhang, F. Xue, J. Tong, W. Guan, B. Wang, J. Solution Chem. **35**, 297 (2006)
8. J.-Z. Yang, J.-S. Gui, X.-M. Lu, Q.-G. Zhang, H.-W. Li, Acta Chim. Sinica **63**, 577 (2005)
9. A. Tekin, J. Safarov, A. Shahverdiyev, E. Hassel, J. Mol. Liquids **136**, 177 (2007)
10. J.G. Huddleston, A.E. Visser, W.M. Reichert, H.D. Willauer, G.A. Broker, R.D. Rogers, Green Chem. **3**, 156 (2001)
11. J. Wang, Y.Tian, Y. Zhao, K. Zhuo, Green Chem. **5**, 618 (2003)
12. C.P. Fredlake, J.M. Crosthwaite, D.G. Hert, S.N.V.K. Aki, J.F. Brennecke, J. Chem. Eng. Data **49**, 965 (2004)
13. H. Tokuda, K. Hayamizu, K. Ishii, M.A.B.H. Susan, M. Watanabe, J. Phys. Chem. B **108**, 16593 (2004)
14. R.G. de Azevedo, J.M.S.S. Esperanca, V. Najdanovic-Visak, Z.P. Visak, H.J.R. Guedes, M.N. da Ponte, L.P.N.J. Rebelo, J. Chem. Eng. Data **50**, 997 (2005)
15. Q. Zhou, L.-S. Wang, H.-P.J. Chen, J. Chem. Eng. Data **51**, 905 (2006)
16. R.L. Gardas, M.G. Freire, P.J. Carvalho, I.M. Marrucho, I.M.A. Fonseca, A.G.M. Ferreira, J.A.P.J. Coutinho, J. Chem. Eng. Data **52**, 80 (2007)
17. P.A.Z. Suarez, S. Einloft, J.E.L. Dullius, R.F. de Souza, J. Dupont, J. Chim. Phys.-Chim. Biol. **95**, 1626 (1998)
18. R. Hagiwara, Y. Ito, J. Fluorine Chem. **105**, 221 (2000)
19. L.C. Branco, J.N. Rosa, J.J.M. Ramos, C.A.M. Afonso, Chem.-Eur. J. **8**, 3671 (2002)
20. S.K. Kim, B.K. Shin, L. Huen, *Korean.* J. Chem. Eng. **21**, 1010 (2004)
21. K. Seddon, A. Stark, M.-J. Torres, *ACS Symp. Series*, Chap. 4 (2002), p. 34
22. L.P.N. Rebelo, V. Najdanovic-Visak, Z.P. Visak, M. Nunes da Ponte, J. Szydlowski, C.A. Cerdeirina, J. Troncoso, L. Romani, J.M.S.S. Esperanca, H.J.R. Guedes, H.C. deSousa, Green Chem. **6**, 369 (2004)
23. M.T. Zafarani-Moattar, H.J. Shekaari, J. Chem. Thermodyn. **38**, 1377 (2006)
24. T. Nishida, Y. Tashiro, M. Yamamoto, J. Fluorine Chem. **120**, 135 (2003)
25. Y.A. Sanmamed, D. Gonzalez-Salagado, J. Troncoso, C.A. Cerdeirina, L. Romani, Fluid Phase Equilib. **252**, 96 (2007)
26. S.N.V.K. Aki, B.R. Mellein, E.M. Saurer, J.F. Brennecke, J. Phys. Chem. B **108**, 20355 (2004)
27. J.N.C. Lopes, T.C. Cordeiro, J.M.S.S. Esperanca, H.J.R. Guedes, S. Huq, L.P.N. Rebelo, K.R. Seddon, J. Phys. Chem. **109**, 3519 (2005)
28. W. Wagner, A. Pruß, J. Phys. Chem. Ref. Data **31**, 387 (2002)
29. K.M. de Reuck, R.J.B. Craven, *Methanol International Thermodynamic Tables of the Fluid State-12* (Blackwell Scientific, Oxford, 1993)

30. I.M. Abdulagatov, A. Tekin, J. Safarov, A. Shahverdiyev, E. Hassel, J. Sol. Chem. (in press)
31. E.C. Ihmels, J. Gmehling, Ind. Eng. Chem. Res. **40**, 4470 (2001)
32. M.J. Assael, J.H. Dymond, D. Exadaktilou, Int. J. Thermophys. **15**, 155 (1994)
33. J.H. Dymond, R. Malhotra, Int. J. Thermophys. **8**, 541 (1987)
34. J.H. Dymond, R. Malhotra, Int. J. Thermophys. **8**, 941 (1988)
35. A. Kumagai, K. Date, H. Iwasaki, J. Chem. Eng. Data **21**, 226 (1976)
36. J.A. Widegren, A. Laesecke, J.W. Magee, Chem. Comm. 1610 (2005)
37. K.N. Marsh, J.A. Boxall, R. Lichtenthaler, Fluid Phase Equilib. **219**, 93 (2004)
38. M.E. Van Valkenburg, R.L. Vaughn, M. Williams, J.S. Wilkes, Thermochim. Acta **425**, 181 (2005)
39. A. Dominguez-Vidal, N. Kaun, M.J. Ayora-Canada, B. Lendl, J. Phys. Chem. B **111**, 4446 (2007)
40. M.L. Japas, J.L. Alvarez, J. Kukuljan, K. Gutkowski, R. Fernández-Prini, in *Steam, Water, and Hydrothermal Systems: Proc. 13th Int. Conf. Prop. Water and Steam*, ed. by P.R. Tremaine, Ph.G. Hill, D.E. Irish, P.V. Balakrishnan (NRC Research Press, Ottawa, 2000), pp. 165–174
41. H.E. Dillon, S.G. Penoncello, Int. J. Thermophys. **25**, 321 (2004)
42. I.M. Abdulagatov, N.D. Azizov, J. Therm. Anal. Calorim. **87**, 483 (2007)
43. I.M. Abdulagatov, N.D. Azizov, J. Chem. Thermodyn. **38**, 1402 (2006)
44. I.M. Abdulagatov, N.D. Azizov, Int. J. Thermophys. **24**, 1581 (2003)
45. O. Redlich, D.M. Mayer, Chem. Rev. **64**, 221 (1964)
46. A. Roux, G.M. Musbally, G. Perron, J.E. Desnoyers, Can. J. Chem. **56**, 24 (1978)
47. Y. Hiejima, M. Yao, J. Chem. Phys. **119**, 7931 (2003)
48. J.M.H. Levelt Sengers, G. Morrison, G. Nielson, R.F. Chang, C.M. Everhart, Int. J. Thermophys. **7**, 231 (1986)
49. J.M.H. Levelt Sengers, J. Supercrit. Fluids **4**, 215 (1991)
50. R.F. Chang, J.M.H. Levelt Sengers, J. Phys. Chem. **90**, 5921 (1986)
51. A.A. Chialvo, P.T. Cummings, AIChE J. **40**, 1 558 (1994)
52. P.G. Debenedetti, R.S. Mohamed, J. Chem. Phys. **90**, 4528 (1989)
53. J.M.H. Levelt Sengers, in *Supercritical Fluids: Fundamentals for Applications*, ed. by E. Kiran, J.M.H. Levelt Sengers (Kluwer, Dordrecht, 1994), pp. 3–38
54. R. Fernández-Prini, M.L. Japas, Chem. Soc. Rev. **23**, 155 (1994)
55. J.P. O'Connell, Y. Hu, K.A. Marshall, Fluid Phase Equilib. **158**, 583 (1999)
56. E.Z. Hamod, G.A. Manssori, in *Fluctuation Theory of Mixtures*, ed. by E. Matteoli, G.A. Manssori (Taylor and Francis, New York, 1990), pp. 95–130
57. D.B. McGuigan, P.A. Monson, Fluid Phase Equilib. **57**, 227 (1990)
58. A.A. Chialvo, P.T. Cummings, AIChE J. **44**, 667 (1998)
59. J.P. O'Connell, Mol. Phys. **20**, 27 (1971)
60. P.T. Cummings, A.A. Chialvo, Chem. Eng. Sci. **49**, 2735 (1994)